IEEE Access
Multidisciplinary ⋮ Rapid Review ⋮ Open Access Journal

Received May 25, 2020, accepted June 14, 2020, date of publication June 19, 2020, date of current version June 30, 2020.

Digital Object Identifier 10.1109/ACCESS.2020.3003740

Construction and Analysis of Two-Dimensional Axisymmetric Model of Electromagnetic Tube Bulging With Field Shaper

LI QIU[1,2], (Member, IEEE), KUI DENG[1], AHMED ABU-SIADA[3], (Senior Member, IEEE), QI XIONG[1], (Member, IEEE), NINGXUAN YI[1], YUWEI FAN[1], JINPENG TIAN[1], AND JINBO JIANG[1]

[1]College of Electrical Engineering and New Energy, China Three Gorges University, Yichang 443002, China
[2]Hubei Provincial Key Laboratory for Operation and Control of Cascaded Hydropower Station, Yichang 443002, China
[3]Discipline of Electrical and Computer Engineering, Curtin University, Perth, WA 6102, Australia

Corresponding author: Jinbo Jiang (jinbojiang@163.com)

This work was supported in part by the National Natural Science Foundation of China under Grant 51877122 and Grant 51707104, and in part by the Research Fund for Excellent Dissertation of China Three Gorges University under Grant 2019SSPY065.

ABSTRACT Due to the fact that geometrical structure of tube electromagnetic bulging process with field shaper does not conform to the axisymmetric property, three-dimensional (3D) model is usually used to analyze the process which is complicated and time consuming. Therefore, on the basis of understanding the working principle of the field shaper, a two-dimensional (2D) model with current constraint is proposed in this paper to analyze the electromagnetic bulging process of a tube fitted with a field shaper. COMSOL finite element analysis software is used to develop three models for performance analysis and comparison, these are: conventional 3D model and the proposed 2D model with and without current constraint. Simulation results show that the induced eddy current density, magnetic flux density and electromagnetic body density of the two-dimensional model with current constraint are in good agreement with the results of the three-dimensional model. This provides an alternative and effective way to analyze the performance of the tube electromagnetic bulging with field shaper using a simple but yet reliable 2D model.

INDEX TERMS Electromagnetic forming, field shaper, lightweight alloy, finite element analysis.

I. INTRODUCTION

Application of lightweight alloy materials in aviation, aerospace and automobile industry has been given much attention in the last two decades [1]–[3]. However, because of its poor plasticity at room temperature, light alloy processing using traditional machining technology calls for a substantial improvement [4]–[6].

Electromagnetic forming (EMF) is a kind of high-speed forming technology which employs pulse electromagnetic force to process material forming [7]–[9]. This technology has been widely utilized due to its ability to improve the formability of light alloy materials [10]–[13]. Field shaper is a common auxiliary part in the electromagnetic forming process which is usually placed between the driving coil and the workpiece to adjust the magnetic field distribution and hence the generated electromagnetic force [14]–[16].

Majority of the current research in EMF with field shaper is based on experimental measurements or 3D simulation model [17]–[19]. In [20], the bulging effect of the workpiece under field shapers of different materials and geometrical dimensions is studied experimentally to select the optimum field shaper material and dimensions. In [21], a three-dimensional numerical model of a multi turns coil field shaper and AL6061-T6 pipe fitting is developed. In the experimental analysis, photonic Doppler velocimetry (PDV) is usually used to measure the forming speed accurately which increases the cost. As such, due to the high cost of the experimental-based study and the complexity of the 3D simulation model, a few studies have proposed a two-dimensional model. In [22], one eighth two-dimensional axisymmetric model with field shaper is developed using ANSYS software. Reported results attest that the field shaper

The associate editor coordinating the review of this manuscript and approving it for publication was Ildiko Peter.

can effectively improve the radial force in tube compression (bulging). In [23], 2D and 3D models are developed to investigate the influence of the field shaper parameters on the magnetic field and the electromagnetic force distributions on the workpiece. However, the physical construction of the so far proposed two-dimensional models in the literature is not clear enough, with lack of reasonable field shaper modelling.

Based on the principle of electromagnetic tube bulging, a 2D axisymmetric simulation model of electromagnetic tube bulging with field shaper is proposed in this paper by introducing current coupling constraint in the region of the field shaper. COMSOL finite element analysis software is used to simulate the proposed model. To validate the robustness of the proposed 2D model, three models are developed and compared these are, 3D model and 2D model with and without current constraint. The parameters of the three models including flux density, induced eddy current of the field shaper and electromagnetic force distribution are analyzed as elaborated below.

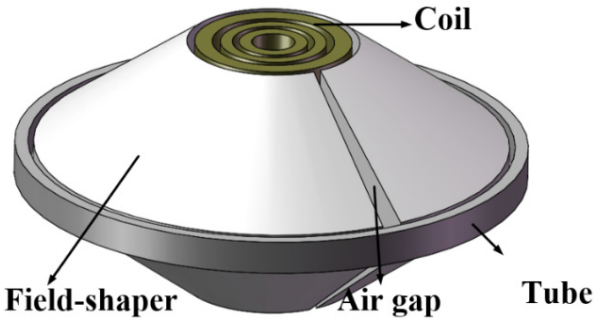

FIGURE 1. Electromagnetic bulging structure of tube with field shaper.

II. PRINCIPLE OF ELECTROMAGNETIC TUBE BULGING WITH FIELD SHAPER

The electromagnetic bulging structure of a tube with field shaper is shown in Figure 1, of which the driving coil, field shaper and tube are placed concentrically from inside to outside with air gap along the axial direction of the field shaper. This structure significantly concentrates the force on the tube.

When a pulse current is applied to the driving coil, induced eddy current will be generated on the field shaper. Because of the air gap, the induced eddy current in the field shaper does not form a closed circuit. On the other hand, because the length of the outer wall of the field shaper is smaller than that of the inner wall (see Figure 2(b)), the current and flux densities of the outer wall of the field shaper are enhanced. The current on the outer wall of the field shaper generates induced eddy current on the tube. The pulse electromagnetic force generated due to the interaction between this eddy current and the magnetic flux drives the tube to accelerate to realize the required forming.

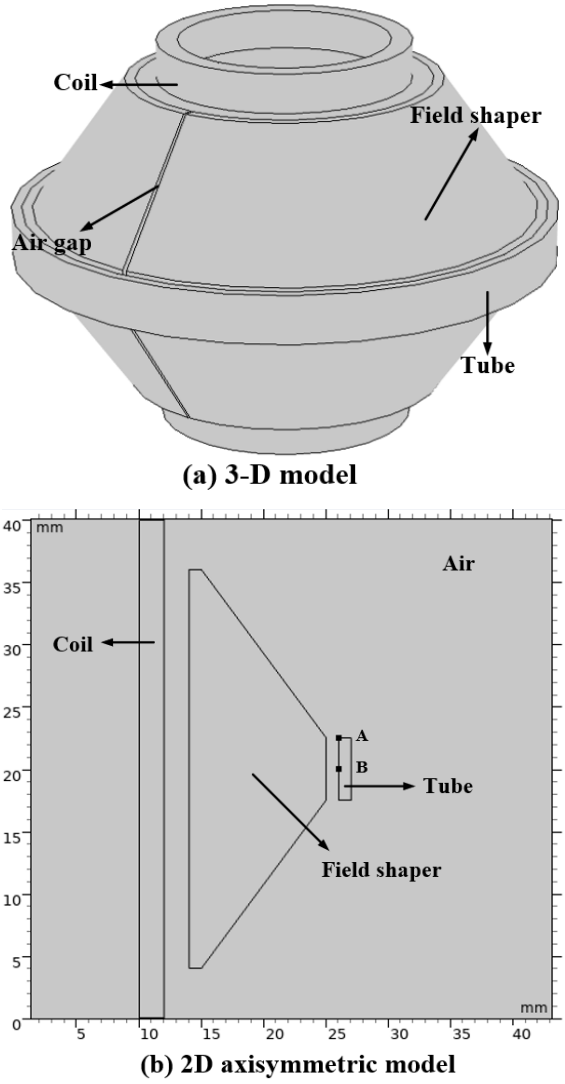

FIGURE 2. Geometric model (a) 3D model; (b) 2D model.

III. FINITE ELEMENT ANALYSIS

While the driving coil and tube are of axisymmetric geometrical structure, electromagnetic bulging of the tube with field shaper cannot be directly simplified into a 2D model because of the air gap and the non-axisymmetric structure of the field shaper. The key contributions of this paper is the presentation of a simplified 2D model for tube electromagnetic bulging with field shaper without compromising the model accuracy. Table 1 shows the basic parameters of the main components of the proposed model. The pulse current source of the driving coil is a damped sinusoid waveform of 5kA amplitude and 160μs width. For accurate comparison, parameters in Table 1 are used to build three models; 3D and 2D model with and without current constraint using finite element analysis as elaborated below.

A. THREE-DIMENSIONAL MODEL

To emulate the actual electromagnetic tube bulging with field shaper, a 3D model is developed with the inclusion of the

TABLE 1. Basic parameters of the proposed model.

	coil	Field shaper	tube
Outer radius (mm)	12	25	27
Internal radius (mm)	10	14	26
Height of coil side (mm)	40	32	5
Height of tube side （mm）	-	5	-
Materials	copper	Rad copper	Aluminum
Conductivity (10^7S/m)	5.7	4.52	3.53
Relative permeability (H/m)	1	1	1

driving coil, field shaper, tube and surrounding air layer, as shown in Fig. 2(a) (air layer is not shown). The 3D model can effectively reflect the tube electromagnetic bulging process with field shaper. This 3D model is used as a reference to assess the performance of the proposed 2D model. The three-dimensional model is executed in a 28min and 28s and takes 4.05GB physical memory and 4.52GB virtual memory.

B. TWO-DIMENSIONAL MODEL WITHOUT CURRENT CONSTRAINT

Ignoring the influence of air gap, the field shaper is regarded as a closed conductor ring of axisymmetric structure, and the electromagnetic bulging of the tube with the field shaper can be simplified into a 2D axisymmetric model, as shown in Fig. 2(b). Although of the small geometrical dimensions of the air gap, its existence is essential to control the flow of the induced eddy current in the field shaper. As such it cannot be ignored in the simulated model. This model does not consider the current constraint and is used for comparison analysis.

C. PROPOSED TWO-DIMENSIONAL MODEL WITH CURRENT CONSTRAINT

In order to simplify the electromagnetic bulging of tube with field shaper into a feasible 2D model, the induced eddy current in the field shaper must be restricted. The induced eddy current comprises four components: I_1 on the inner wall of the field shaper, I_2 on one side of the air gap, I_3 on the outer wall of the field shaper and I_4 on the other side of the air gap, as shown in Figure 3(a). To simplify the finite element simulation model, the air gap is filled with the same conductor material, as shown in Figure 3(b). As I2 and I4 are of the same magnitude and opposite direction, the magnetic field generated by these currents is only constrained in the vicinity of the air gap. Thus the influence on these two current components on the electromagnetic bulging of the whole tube can be ignored, so the model can be further simplified as shown in Figure 3(c). In this case, the current collector is axisymmetric both in structure and current distribution, and it can be simplified into a 2D-model. The current constraint is considered in the simplified model by controlling the current components on the inner and outer walls of the field shaper to be of equal magnitudes and opposite directions. In the actual modeling, this constraint is set by adjusting the total current in the collector to zero. The calculation time for the proposed two-dimensional model, is only 4s and it takes only 0.98GB of the physical memory and 1.2GB of the virtual memory. This is a significant reduction from the time and memory required to solve the 3D model as reported above.

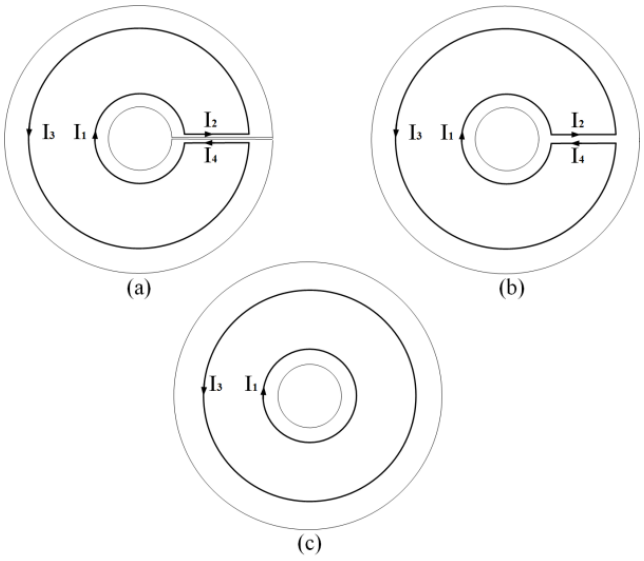

FIGURE 3. Equivalent process of the filed shaper model. (a) Initial model; (b) Model after filling; (c) Final model.

D. SETTING OF PHYSICAL CONDITIONS OF FINITE ELEMENT MODEL

A pulse current is applied to the driving coil to generate a pulse magnetic field as per the equation below:

$$\nabla \times \boldsymbol{H} = \boldsymbol{J} \tag{1}$$

where $\boldsymbol{H}$ is the magnetic field strength, $\boldsymbol{J}$ is the external current density, obtained by dividing the pulse current $\boldsymbol{I}$ of the driving coil by the cross-sectional area of the coil.

In the filed shaper, there is no external current, but there is an electric field intensity generated by the change of the magnetic flux as below:

$$\nabla \times \boldsymbol{E} = -\frac{\partial \boldsymbol{B}}{\partial t} \tag{2}$$

$$\boldsymbol{J_e} = \sigma \boldsymbol{E} \tag{3}$$

where $\boldsymbol{E}$ is the intensity of the induced electric field in the collector, $\boldsymbol{B}$ is the flux density, $\boldsymbol{J_e}$ is the induced current density in the collector, and σ is the conductivity of the collector.

For a 2D-model with current constraint, $(\boldsymbol{I} = 0)$;

$$\int_s \boldsymbol{J_e} \cdot d\boldsymbol{S} = 0 \tag{4}$$

where $\boldsymbol{S}$ is the collector cross sectional-area. Similar to the collector, there is no external current in the tube and the

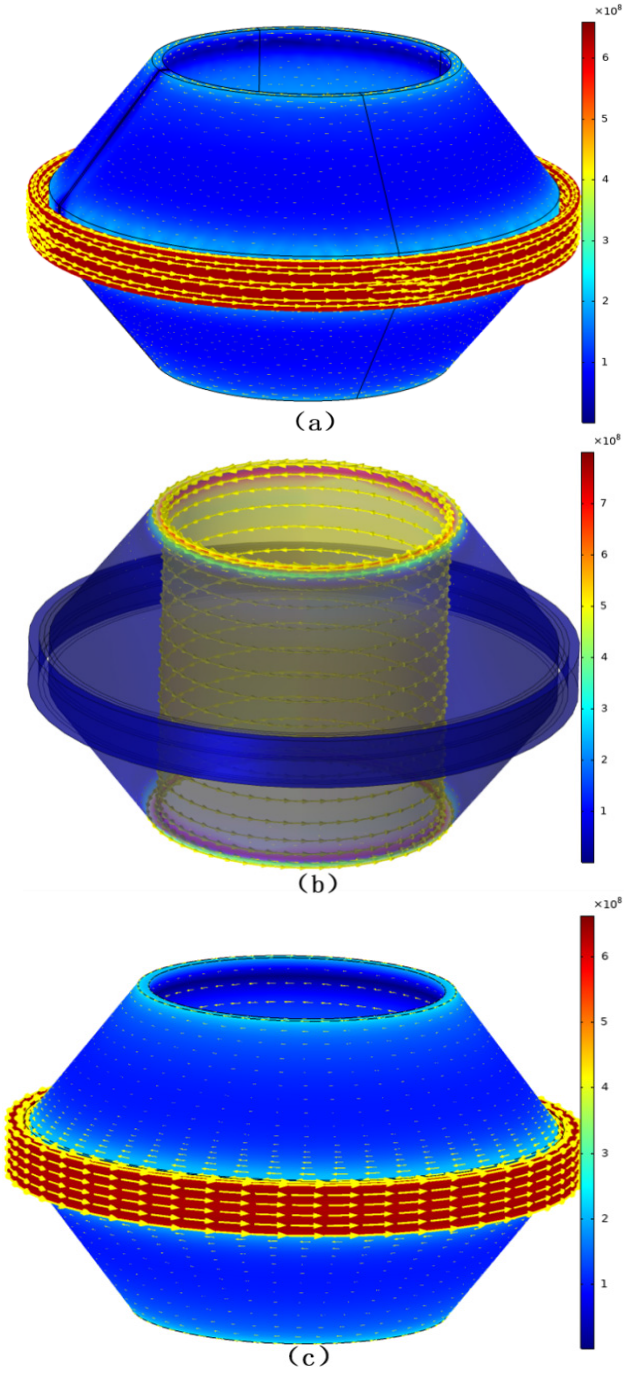

FIGURE 4. Current density (A/m^2) of the 3 investigated models (a) 3D-model, (b) 2D- model without current constraint, (c) proposed 2D-model with current constraint.

electric field intensity is generated due to the change of the magnetic flux that results in induced eddy current in the tube.

The electromagnetic force on the tube is calculated from:

$$\boldsymbol{F} = \boldsymbol{J_e} \times \boldsymbol{B} \tag{5}$$

Since the current components on the inner and outer walls of the collector are equal in magnitude and opposite in direction, the skin depth δ can be calculated based on the below equation.

$$\delta = \sqrt{\frac{2}{\omega\mu\mu_0\sigma}} \tag{6}$$

where ω is the angular velocity, μ is the permeability, μ_0 is the vacuum permeability, σ is the conductivity.

In the developed model, the current frequency is 3.125 kHz and the skin depth calculated using (6) is 1.14mm.

IV. SIMULATION RESULTS

In order to validate the robustness of the simplified 2D-model, this section analyzes and compares the performance of the three models mentioned above in terms of the induced eddy current, flux density, and the electromagnetic force distribution.

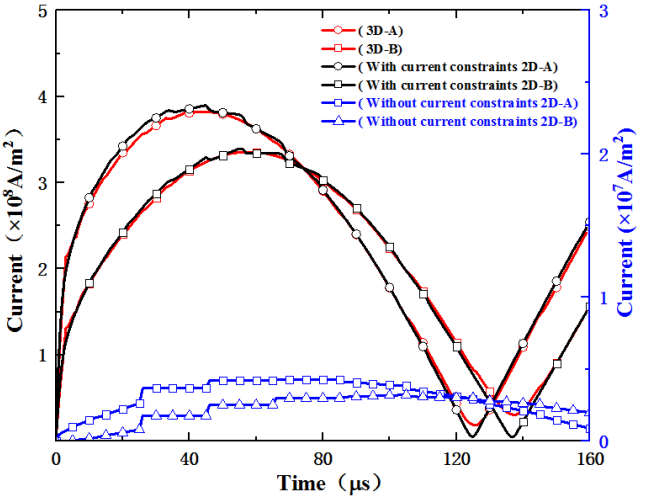

FIGURE 5. Eddy current density waveforms at points A and B of the tube for the 3 investigated models.

Figure 4 shows the current distribution of the tube electromagnetic bulging with field shaper for the three investigated models. To enhance the clarity of the results, the current density of the 2D-models is rotated 360°.

It can be observed that the induced eddy current on the inner wall of the field shaper of the 3D-model exhibits a counterclockwise distribution. When the eddy current encounters the air gap, it transits to the outer wall of the field shaper and exhibits a clockwise distribution after which it flows back to the inner wall along the other side of the air gap. Distribution of the induced eddy current in the tube is in anticlockwise direction, and the induced eddy current density is clearly enhanced. It is to be noted that in Figures 4 (a) and (c), the arrow of the outermost layer of the pipe fitting is in counterclockwise direction.

In the 2D-model without current constraint (Figure 4(b)), the induced eddy current of the field shaper is almost distributed only on the inner wall of the field shaper and it exhibits a clockwise direction. Because there is no current constraint, the field shaper in this case is equivalent to a continuous conductor and the distribution of the eddy current

is inconsistent with the actual situation. The field shaper acts as a shield, resulting in almost no induced eddy current on the tube.

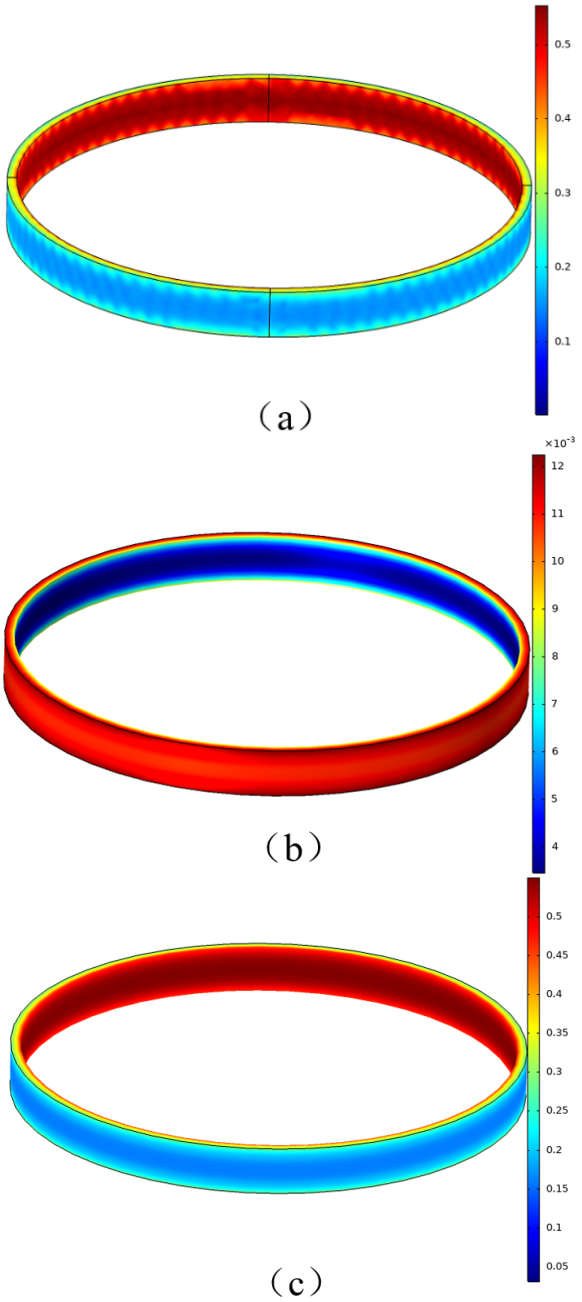

FIGURE 6. Cloud chart of the magnetic flux density (T) distribution across the tube. (a) 3D-model; (b) 2D-model without current constraint; (c) proposed 2D-model with current constraint.

In the proposed 2D-model with current constraint, except that there is no air gap, the distribution of the induced eddy current in the field shaper and the tube as shown in Figure 4(c) is similar to that of the 3D-model shown in Figure 4(a). To clarify the obtained results, the eddy current density at two arbitrary points A and B at the end and middle of the tube (As shown in Figure 2) is measured for the 3 investigated

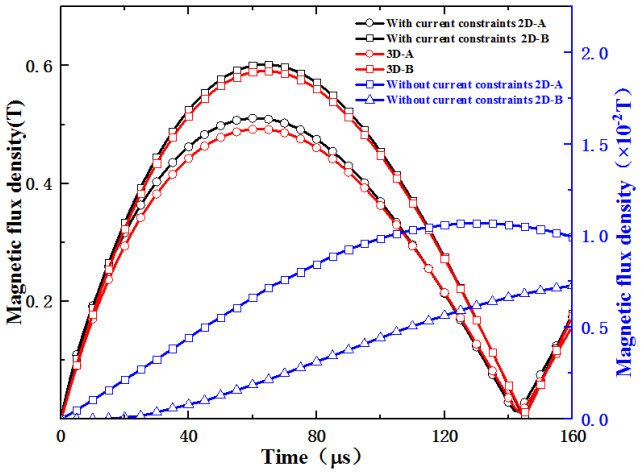

FIGURE 7. Magnetic flux density waveform at points A and B of the tube for the 3 investigated models.

models. It can be observed from the results shown in Figure 5 that the generated eddy current density at the selected two points of the 3D-model and the proposed 2D-model with current constraint are of good agreement. For both models, the maximum amplitude of the eddy current density at point A is 3.89×10^8 A/m^2 while the maximum eddy current density at the same point for a 2D-model without current constraint is 4.27×10^6 A/m^2. Because of the concentration of induced eddy current at the end of the tube, the density of the induced eddy current at point A is higher than that at point B. The magnetic flux density and the induced eddy current interact to produce the electromagnetic force. Figure 6 shows the cloud chart of the magnetic flux density distribution across the tube. Similar to the current density distribution, the magnetic flux density of the 3D-model and that of the proposed 2D-model with current constraint are of similar trend that is far different from the current-free 2D model. The mesh division of the 3D-model is not detailed enough. As such its cloud image is not exactly coinciding with that of the 2D-model with current constraint.

The flux density waveforms at points A and B of the tube for the investigated 3 models are shown in Figure 7. It can be seen that the maximum amplitude of the flux density of the 3D- model and the 2D-model with current constraint is 0.55T, while the maximum flux density in the 2D-model without current constraint is 0.11T.

Figure 8 shows cloud charts of the electromagnetic force volume density distribution of the tube for the 3 investigated models. It can be also observed that the cloud chart of the 3D-model is consistent with the cloud chart of the proposed 2D-model with current constraint. Results also show that the electromagnetic force density on the inner wall is significantly greater than that on the outer wall. This is consistent with the distribution of the induced eddy current density on the tube shown in Figure 6, which is caused due to the skin effect. On the other hand, the electromagnetic force distribution on the tube without current constraint is obviously inconsistent with the other 2 models. Figure 9 shows the distribution

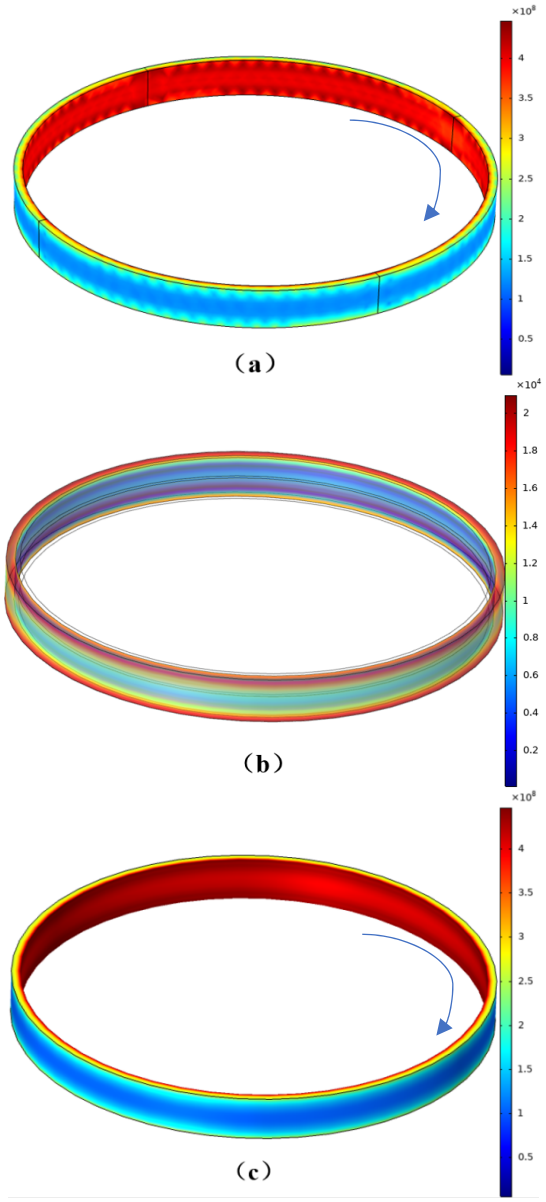

FIGURE 8. Cloud chart of the electromagnetic force density distribution of the tube (x10^8 N/m^3) (a) 3D-model, (b) 2D-model without current constraint, (c) 2D-model with current constraint.

of the electromagnetic force bulk density with time at the selected two points A and B on the tube. Again, Figure 9 attest the previously obtained results and validate the consistent performance of the proposed simplified 2D-model with the conventional 3D model.

V. CONCLUSION

In order to solve the complexity of the tube electromagnetic bulging simulation with field shaper, a simplified two-dimensional model with current constraint is proposed in this paper based on the distribution characteristics of the induced eddy current in the field shaper. Detailed comparative analysis of three models including conventional 3D-model, 2D-model without current constraint and the proposed 2D-model with current constraint in terms of

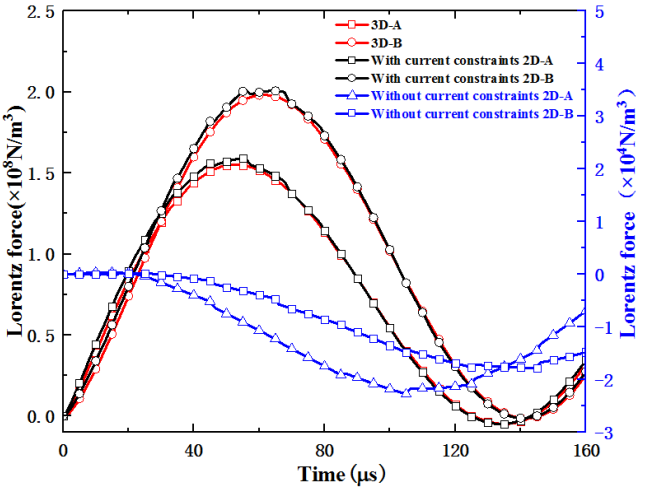

FIGURE 9. Electromagnetic force bulk density waveform at points A and B of the tube for the 3 investigated models.

induced eddy current density, magnetic flux density and electromagnetic force volume density is conducted. Results reveal the consistent performance of the proposed simplified 2D-model and the conventionally used 3D-model. The simplified model can be executed in a few seconds whereas the 3D model takes more than 28 min to be executed. This validates the feasibility of the simplified simulation model to emulate the real operation of the tube electromagnetic bulging with field shaper. The proposed model is simple, accurate and easy to implement which opens the door for further research in the area of tube electromagnetic forming technology.

REFERENCES

[1] Q. Cao, L. Du, Z. Li, Z. Lai, Z. Li, M. Chen, X. Li, S. Xu, Q. Chen, X. Han, and L. Li, "Investigation of the Lorentz-force-driven sheet metal stamping process for cylindrical cup forming," *J. Mater. Process. Technol.*, vol. 271, pp. 532–541, Sep. 2019.

[2] Q. Xiong, H. Tang, C. Deng, L. Li, and L. Qiu, "Electromagnetic attraction-based bulge forming in small tubes: Fundamentals and simulations," *IEEE Trans. Appl. Supercond.*, vol. 28, no. 3, pp. 1–5, Apr. 2018.

[3] L. Qiu, Y. J. Yu, X. P. Nie, Y. Q. Yang, and P. Su, "Study on material deformation performance and electromagnetic force loading in electromagnetic tube expansion process," *Trans. China Electrotech. Soc.*, vol. 34, no. 2, pp. 212–218, 2019.

[4] L. Qiu, W. Zhang, A. Abu-Siada, G. Liu, C. Wang, Y. Wang, B. Wang, Y. Li, and Y. Yu, "Analysis of electromagnetic force and formability of tube electromagnetic bulging based on convex coil," *IEEE Access*, vol. 8, pp. 33215–33222, 2020, doi: 10.1109/ACCESS.2020.2974758.

[5] L. Qiu, Q. Cao, W. Zhang, A. Abu-Siada, Q. Xiong, C. Wang, Y. Xiao, B. Wang, Y. Li, and J. Jiang, "Electromagnetic force distribution and wall thickness reduction of three-coil electromagnetic tube bulging with axial compression," *IEEE Access*, vol. 8, pp. 21665–21675, 2020, doi: 10.1109/ACCESS.2020.2969678.

[6] L. Qiu, C. Wang, A. Abu-Siada, Q. Xiong, W. Zhang, B. Wang, N. Yi, Y. Li, and Q. Cao, "Coil temperature rise and workpiece forming efficiency of electromagnetic forming based on half-wave current method," *IEEE Access*, vol. 8, pp. 9371–9379, 2020, doi: 10.1109/ACCESS.2020.2965254.

[7] L. Qiu, Y. Yu, Y. Yang, X. Nie, Y. Xiao, Y. Ning, F. Wang, and C. Cao, "Analysis of electromagnetic force and experiments in electromagnetic forming with local loading," *Int. J. Appl. Electromagn. Mech.*, vol. 57, no. 1, pp. 29–37, Apr. 2018.

[8] L. Qiu, K. Deng, Y. Li, X. Tian, Q. Xiong, P. Chang, P. Su, and L. Huang, "Analysis of coil temperature rise in electromagnetic forming with coupled cooling method," *Int. J. Appl. Electromagn. Mech.*, vol. 63, no. 1, pp. 45–58, May 2020, doi: 10.3233/JAE-190062.

[9] Q. Xiong, H. Huang, L. Xia, H. Tang, and L. Qiu, "A research based on advance dual-coil electromagnetic forming method on flanging of small-size tubes," *Int. J. Adv. Manuf. Technol.*, vol. 102, nos. 9–12, pp. 4087–4094, Jun. 2019.
[10] Q. Cao, Z. Lai, Q. Xiong, Q. Chen, T. Ding, X. Han, and L. Li, "Electromagnetic attractive forming of sheet metals by means of a dual-frequency discharge current: Design and implementation," *Int. J. Adv. Manuf. Technol.*, vol. 90, nos. 1–4, pp. 309–316, Apr. 2017.
[11] L. Qiu, Y. Xiao, C. Deng, Z. Li, Y. Xu, Z. Li, and P. Chang, "Electromagnetic-structural analysis and improved loose coupling method in electromagnetic forming process," *Int. J. Adv. Manuf. Technol.*, vol. 89, nos. 1–4, pp. 701–710, Mar. 2017.
[12] L. Qiu, X. Han, T. Peng, H. Ding, Q. Xiong, Z. Zhou, C. Jiang, Y. Lv, and L. Li, "Design and experiments of a high field electromagnetic forming system," *IEEE Trans. Appl. Supercond.*, vol. 22, no. 3, p. 3700504, Jun. 2012.
[13] Q. Cao, X. Han, Z. Lai, Q. Xiong, X. Zhang, Q. Chen, H. Xiao, and L. Li, "Analysis and reduction of coil temperature rise in electromagnetic forming," *J. Mater. Process. Technol.*, vol. 225, pp. 185–194, Nov. 2015.
[14] L. Qiu, B. Wang, A. Abu-Siada, Q. Xiong, W. Zhang, W. Ge, C. Liu, L. Jiang, and C. Wang, "Research on forming efficiency in double-sheet electromagnetic forming process," *IEEE Access*, vol. 8, pp. 19248–19255, 2020, doi: 10.1109/ACCESS.2020.2968049.
[15] L. Qiu, Y. Yu, Q. Xiong, C. Deng, Q. Cao, X. Han, and L. Li, "Analysis of electromagnetic force and deformation behavior in electromagnetic tube expansion with concave coil based on finite element method," *IEEE Trans. Appl. Supercond.*, vol. 28, no. 3, pp. 1–5, Apr. 2018.
[16] L. Qiu, Y. Yu, Z. Wang, Y. Yang, Y. Yang, and P. Su, "Analysis of electromagnetic force and deformation behavior in electromagnetic forming with different coil systems," *Int. J. Appl. Electromagn. Mech.*, vol. 57, no. 3, pp. 337–345, Jun. 2018.
[17] L. Qiu, Y. Li, Y. Yu, A. Abu-Siada, Q. Xiong, X. Li, L. Li, P. Su, and Q. Cao, "Electromagnetic force distribution and deformation homogeneity of electromagnetic tube expansion with a new concave coil structure," *IEEE Access*, vol. 7, pp. 117107–117114, 2019.
[18] L. Qiu, N. Yi, A. Abu-Siada, J. Tian, Y. Fan, K. Deng, Q. Xiong, and J. Jiang, "Electromagnetic force distribution and forming performance in electromagnetic forming with discretely driven rings," *IEEE Access*, vol. 8, pp. 16166–16173, 2020, doi: 10.1109/ACCESS.2020.2967096.
[19] L. Qiu, Y. Li, Y. Yu, Y. Xiao, P. Su, Q. Xiong, J. Jiang, and L. Li, "Numerical and experimental investigation in electromagnetic tube expansion with axial compression," *Int. J. Adv. Manuf. Technol.*, vol. 104, nos. 5–8, pp. 3045–3051, Oct. 2019.
[20] S. Zhang, A. Nassiri, and B. Kinsey, "Numerical model and experimental investigation of electromagnetic tube compression with field shaper," *Procedia Manuf.*, vol. 26, pp. 537–542, 2018.
[21] H. Yu, C. Li, Z. Zhao, and Z. Li, "Effect of field shaper on magnetic pressure in electromagnetic forming," *J. Mater. Process. Technol.*, vol. 168, no. 2, pp. 245–249, Sep. 2005.
[22] D. H. Wu, T. F. He, X. H. Wang, and Q. Sun, "Analytical modeling and analysis of mutual inductance coupling of rectangular spiral coils in inductive power transfer," *Trans. China Electrotech. Soc.*, vol. 33, no. 3, pp. 680–688, 2018.
[23] M. Jianhua, W. Bo, C. Xiaohui, and H. Wenzhi, "Simulation of working principle of magnetic collector in sheet metal electromagnetic forming," *J. Plastic Eng.*, vol. 18, no. 1, pp. 36–42, 2011.

LI QIU (Member, IEEE) received the B.S., M.S., and Ph.D. degrees in electrical engineering from the Huazhong University of Science and Technology, Wuhan, China, in 2012.

He is currently an Associate Professor with the College of Electrical Engineering and New Energy, China Three Gorges University, Yichang. He is the author of more than 15 articles and more than ten inventions. His research interests include the technology of pulsed high magnetic field, high voltage technology, and electromagnetic forming. He is a Periodical Reviewer of the IEEE TRANSACTIONS ON APPLIED SUPERCONDUCTIVITY and *International Journal of Applied Electromagnetics and Mechanics*.

KUI DENG is currently a Graduate Student majoring in electrical engineering at the College of Electrical Engineering and New Energy, China Three Gorges University, Yichang.

AHMED ABU-SIADA (Senior Member, IEEE) received the B.Sc. and M.Sc. degrees from Ain Shams University, Egypt, in 1998, and the Ph.D. degree from Curtin University, Australia, in 2004, both in electrical engineering.

He is currently an Associate Professor and the Discipline Lead of the Electrical and Computer Engineering at Curtin University. His research interests include power electronics, power system stability, condition monitoring, and power quality. He is the Editor-in-Chief of the *International Journal of Electrical and Electronics Engineering* and a regular reviewer of various IEEE TRANSACTIONS. He is the Vice-Chair of the IEEE Computation Intelligence Society, WA Chapter.

QI XIONG (Member, IEEE) received the B.S., M.S., and Ph.D. degrees in electrical engineering from the Huazhong University of Science and Technology, Wuhan, China, in 2016. He is currently a Lecturer with the College of Electrical Engineering and New Energy, China Three Gorges University, Yichang. His research interests include the technology of pulsed high magnetic field, high voltage technology, and electromagnetic forming.

NINGXUAN YI is currently pursuing the degree in electrical engineering with the College of Electrical Engineering and New Energy, China Three Gorges University, Yichang.

YUWEI FAN is currently pursuing the degree in electrical engineering with the College of Electrical Engineering and New Energy, China Three Gorges University, Yichang.

JINPENG TIAN is currently pursuing the degree in electrical engineering with the College of Electrical Engineering and New Energy, China Three Gorges University, Yichang.

JINBO JIANG received the B.S. degree from the College of Mechatronics and Control Engineering, Hubei Normal University, Huangshi, China, in 2010.

He is currently a Lecturer at the College of Electrical Engineering and New Energy, China Three Gorges University, Yichang. His research interests include the technology of pulsed high magnetic field, high voltage technology, and pulsed power technology.